



HAL
open science

Journey Safety Assessment to Urban Aerial Ropeways Transport Systems Based on Continuous Inspection During Operation

Ronald Martinod, Daniel Estepa, Carmen Paris, Alexander Trujillo, Fabio Pineda, Leonel Castañeda, Jorge Restrepo

► **To cite this version:**

Ronald Martinod, Daniel Estepa, Carmen Paris, Alexander Trujillo, Fabio Pineda, et al.. Journey Safety Assessment to Urban Aerial Ropeways Transport Systems Based on Continuous Inspection During Operation. *Journal of Transportation Safety & Security*, 2015, 7 (4), pp.279-290. 10.1080/19439962.2014.942018 . hal-02160147

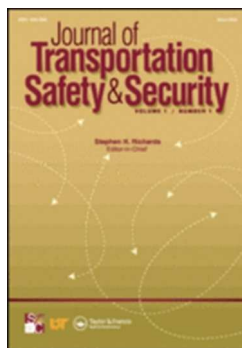
HAL Id: hal-02160147

<https://hal.science/hal-02160147v1>

Submitted on 19 Jun 2019

HAL is a multi-disciplinary open access archive for the deposit and dissemination of scientific research documents, whether they are published or not. The documents may come from teaching and research institutions in France or abroad, or from public or private research centers.

L'archive ouverte pluridisciplinaire **HAL**, est destinée au dépôt et à la diffusion de documents scientifiques de niveau recherche, publiés ou non, émanant des établissements d'enseignement et de recherche français ou étrangers, des laboratoires publics ou privés.



Journey safety assessment to urban aerial ropeways transport systems based on continuous inspection during operation

Journal:	<i>Journal of Transportation Safety & Security</i>
Manuscript ID:	UTSS-2013-0036.R1
Manuscript Type:	Review Article
Date Submitted by the Author:	n/a
Complete List of Authors:	Martinod, Ronald; EAFIT University, Eng. Mechanical Estepa, Daniel; EAFIT University, Eng. Mechanical Paris, Carmen; EAFIT University, Eng. Mechanical Trujillo, Alexander; Empresa de Transporte Masivo del Valle de Aburrá Limitada, Engineering Department Pineda, Fabio; EAFIT University, Eng. Mechanical Castañeda, Leonel; EAFIT University, Eng. Mechanical Restrepo, Jorge; EAFIT University, Eng. Mechanical
Keywords:	Aerial cable car, cable grip, journey safety, strain gauges, urban ropeway system

SCHOLARONE™
Manuscripts

Journey safety assessment to urban aerial ropeways transport systems based on continuous inspection during operation

This paper proposes a continuous inspection method to assess the journey safety applied to aerial cable vehicles of mass transportation; a type of detachable gondola lift in terms of commercial operation in an urban area, specifically referring to the device coupling assembly on the track rope. The inspection method has been developed on the basis of a continual measurement process of the recorded strain conditions on a principal component of the coupling assembly. The selected component is commonly referred to as moving jaw. The proposed inspection procedure is structured based on the following set of consecutive stages: (i) characterization of the load states generated by the commercial operation of the system; (ii) definition of the sections of greater sensitivity to the strains caused by the load states, by means of Finite Elements; (iii) development of a measurement system; (iv) calibration of the measuring system with controlled tests; and (v) implementation and continuous records data in commercial operation.

Keywords: aerial cable car; cable grip; journey safety; strain gauges; urban ropeway system.

1. Introduction

Operators of cable-drawn transport systems must maintain the quality and safety of the service, so they have to inspect periodically the different operation variables of the system (Konieczny and *et.al*, 2008). Bearing in mind that the operating conditions are affected by wear and tear of components, maintenance routines must include the frequent measurement of critical parameters; one of these is the magnitude of the force F_c at the point of coupling between the track rope and the coupling device.

The state of the art has already tackled the measurement of parameters related to the journey safety assessment, by checking the force of the coupling device of the vehicle to the track rope, called cable grip. The cable grip transmits the loads between the aerial cable car and the track rope (Bryja and Knawa, 2011), so it is a critical system:

- In Document FR2750764 a device is described, which verifies the clamping force exerted by the cable grip, formed by two infrared detectors that measure the distance between the moving jaw and some

1
2
3 fixed points in balanced positions of the cable grip (Pomagalski,
4
5
6 1996).

- 7
8 • Document AU2003203595A1 reveals a device to check the clamping
9
10 force, made of at least two different measuring sensors, which are
11
12 arranged in an elastically deformable zone inside a station (Innova,
13
14 2002).

15
16
17 None of the known devices complies with the requirements outlined in this
18
19 paper since the installation of the devices requires that the system has to be stopped
20
21 and then, there are no measurements in operation.
22
23

24
25 The present work proposes: (i) the instrumentation of the cable grip of each
26
27 aerial cable car in order to automatically and continuously inspect the magnitude of
28
29 the clamping force in the whole circuit, travelled by the aerial cable car during the
30
31 commercial operation of the system; (ii) the automatic evaluation of the journey
32
33 safety condition, for implementing an urban transport system of the lift type, which
34
35 creates a high demand for service and high frequency of maintenance routines. In this
36
37 way, it is intended to replace the manual process of the systems safety variables with
38
39 an automated and continuous assessment.
40
41
42

43
44 The proposed inspection method is feasible to be applied to a mass
45
46 transportation system, since it uses sensors (strain gauge arrays) of easy installation
47
48 (Degasperi, 1999), which record reliable signals, and use wireless devices that do not
49
50 interfere with the commercial operation of the system.
51
52

53 54 **2. Description of the object of study**

55
56 This study has been applied to passenger aerial cable cars, which operate in the city of
57
58 Medellin (Colombia). The transport system is similar in design and construction to
59
60 those used for tourist passenger transports in winter regions (e.g. Daemyung–Korea,

1
2
3 La Clusaz–France, Donovaly–Slovakia) (Sever, 2002); it has been manufactured by
4
5 Pomagalski/France, since 2004.
6
7

8 This was the first time an aerial cable was used for urban purpose, completely
9
10 different from a tourist purpose (Mizuma, 2004). Therefore, the transport system is
11
12 required on extreme levels that have not been supported by similar systems, causing
13
14 highly elevated wear rates (Hoffmann, 2006); it will be hence the aerial cable
15
16 transportation system with highest level of demand, in terms of wear hours of
17
18 components and service. Table 1 presents the overall technical characteristics of the
19
20 object of study.
21
22
23

24 The cable grip has the function of clamping (during inter-stations trip) and
25
26 releasing (during transit inside the stations) the aerial cable car to and from the track
27
28 rope, providing the clamping force needed to cancel the relative movements between
29
30 the aerial cable car and the track rope, especially in sections of track with extreme
31
32 slopes (Bryja and Knawa, 2011). Figure 1 shows the main elements of the cable grip,
33
34 defined as the set of basic structural elements that make it up.
35
36
37

38 The development focuses on the study of the recorded load states exerted on
39
40 one of the components of the cable grip, called moving jaw. This element allows the
41
42 grip and release of the clamp onto the track rope and operates in conjunction with two
43
44 coil springs and a fixed jaw. The whole set is articulated through a main shaft, holding
45
46 the aerial cable car due to the force of the springs (Doppelmayr, 1998). The moving
47
48 jaw is made of 36NiCrMo16 material with HB350-390 hardness and resistance to
49
50 stress of 850 MPa, according to the material specifications.
51
52
53

54 Five general operation scenarios have been identified during the commercial
55
56 service of the transport system, which exert different conditions of work to the cable
57
58 grip. The scenarios directly define the load states ξ_i , applied to the moving jaw:
59
60

- ξ_0 load state: it consists of the travel of the vehicle in inter-stations trip. In this state, the vehicle must be fully attached to the track rope. The total weight of the aerial cable car is transmitted from the cable grip to the track rope;
- ξ_1 load state: it is the load state that occurs at the moment when the clamp device comes into contact with a first element in the station, altering its dynamic status.
- ξ_2 load state: it is the load state in which the cable grip gets aligned and leads during the first transit in the station. In this state, the wheels of displacement of the cable grip run on a surface of the station, called stabilization track.
- ξ_3 load state: it is the load state in which the open-close-wheel belonging to the cable grip moves along an element of the station called coil ramp, causing the opening of the gripper and the freeing of the aerial cable car from the track rope.
- ξ_4 load state: it is the load state in which the open-close-wheel belonging to the cable grip is at its maximum displacement, causing the greatest opening of the gripper. In this state the aerial cable car is completely released from the track rope.

{Figure 1}

{Table 1}

3. Determination of the inspection point on the coupling device

The determination of the inspection point on the cable grip is done by an analysis of the distribution of stress-strain in the moving jaw, generated at each of the load states

1
2
3
4 ξ_i whit $i = \{0, \dots, 4\}$, the load state ξ_0 is sensitive to external conditions (Degasperri,
5
6 1999): (i) terms and conditions of operation –live loads, operation frequency–; (ii)
7
8 environmental conditions –wind loads, temperature, moisture, corrosion, etc.–; and
9
10 (iii) system availability. However, the load state ξ_0 can be considered a quasi-static
11
12 load in the event of the load state ξ_0 is made in controlled tests, which has been
13
14 performed in quasi-static conditions, i.e. then the controlled test has the following
15
16 features: (i) a null live load; (ii) a constant travel speed; (iii) a negligible wind load;
17
18 (iii) a constant temperature and moisture.

19
20
21
22
23
24 The analysis of the stress-strain distribution was performed with Finite Elements
25
26 Method (FE) using a linear elastic model with the integration algorithms developed by
27
28 Ansys®. FE is used to simulate the particular characteristics of the moving jaw, and is
29
30 considered as a true virtual prototype. Virtual techniques allow the model to generate
31
32 information on the behaviour of the moving jaw in each of the load states ξ_i , so that
33
34 they are comparable only with physical prototypes. For the construction of the model
35
36 in FE, it is necessary to pose the static elastic problem.

3.1. Development of the FE model

37
38
39
40
41
42
43
44
45 The elastic model with FE allows analysing the strain and stress distribution in a solid
46
47 element based on the principle of Minimum Potential Energy (MPE). The MPE
48
49 establishes that the displacement $\{u\}$ that comply with the differential equations of
50
51 equilibrium, as well as the surface boundary conditions, give a minimum for the total
52
53 potential energy in comparison with any other field of displacement that satisfy the
54
55 same boundary conditions. For an isotropic material in the elastic range, the
56
57 relationship holds true $\{\sigma\} = [D]\{\epsilon\}$, where $[D]$ is the stiffness symmetric matrix of
58
59
60

1
2
3 the material which is written in terms of the E and ν constants, and represents the
4 modulus of elasticity and Poisson, respectively. The FE solution assumes that the
5
6 modulus of elasticity and Poisson, respectively. The FE solution assumes that the
7 displacement function in small areas of the component can be expressed depending on
8
9 the displacement of the element in the nodes, this is $\{u\} = \sum_{i=1}^q [N]_{(x,y,z)} \{u\}_i$, where,
10
11 $[N]_{(x,y,z)}$, is the interpolation matrix function, and q is the number of nodes that are
12
13 considered in the element.
14
15
16

17
18 The analysis process starts with the geometric modelling, using a three-dimensional
19
20 model generated by using a CAD tool. The FE model is built with the following
21
22 assumptions: (i) the geometric details that do not influence the transmission of load
23
24 are omitted; (ii) the non-linear components in the geometry of the model are
25
26 negligible in the system; (iii) the displacements are performed in the elastic region of
27
28 the material; (iv) the stress that are external to the areas of interest are not considered.
29
30
31

32 It is assumed that the magnitude of the mass of the moving jaw, m_t , is
33
34 negligible in relation to the charges that flow at the clamp device. Therefore, it is
35
36 possible to express $m_t \cong 0$, and the inertia matrix will be $\{I_t\} \cong \{0\}$. Accordingly, for
37
38 each ξ_i it is possible to consider the system of equilibrium equations as $\sum\{P\} = m_t \cdot$
39
40 $\vec{a}_t = \vec{0}$, and $\sum\{M\} = \{I_t\} \cdot \vec{\rho}_t = \vec{0}$, where \vec{a}_t and $\vec{\rho}_t$ denote translational and rotational
41
42 acceleration respectively.
43
44
45
46

47 A procedure is carried out to find the equations of equilibrium of the system
48
49 (Bryja and Knawa, 2011; Petrova and *et.al*, 2011), which can be obtained through any
50
51 of the classical methods defined in the mechanics of solid bodies –e.g. free body
52
53 diagram– (Liedl, 1999), finding $\{P\}$ and $\{M\}$ at each ξ_i , thus defining the FE model
54
55 boundary conditions. Appendix 2 describes in detail the boundary conditions of the
56
57 FE model for each ξ_i . Table 2 shows that the load states, where there are the greatest
58
59
60

magnitudes of force, correspond to ξ_0 and ξ_4 , the task will therefore focus on the analysis of the force at these load states.

3.2. Selection of the measuring point for inspection of the clamping force

It has been established a set of criteria to select a suitable measuring point in the moving jaw for the different ξ_i : (i) the measurement point must be accessible to the instrumentation; (ii) the measurement point must be such that the instrumentation does not interfere with the operation of the system; (iii) the measurement point must be located at a superficial point with a sufficient sensitivity range, so that an arrangement of strain gauges can properly register the strain.

Based on the results of the FE model (see Appendix 3), the measurement point P , is chosen for the installation of the strain gauge array. P clearly complies with criteria (i) and (ii) is noticeable in the different ξ_i . The spatial location of P in the moving jaw is shown in Figure 2.

{Figure 2}

4. Development of a measuring system under operating conditions

A measuring arrangement is set at point P to continuously estimate the magnitudes and directions of the strains $\{\varepsilon_r, \varepsilon_s, \varepsilon_t\}$ in three reference axes r, s, t (see Figure 3.a). This is done using a strain gauge array (resistive sensors sensitive to the variation of deformation) attached to the surface of the moving jaw in the point P . The recorded values $\{\varepsilon_r, \varepsilon_s, \varepsilon_t\}$ are wirelessly transmitted to a data acquisition system, to process data in real time.

Based on $\{\varepsilon_r, \varepsilon_s, \varepsilon_t\}$, it is possible to calculate the magnitudes of the normal strains $\{\varepsilon_1, \varepsilon_2\}$, and shear strain $\{\gamma_{12}\}$ on two axes, 1 and 2 (see Figure 3.b), by means

of methods of linear transformation. The solution to the posing of transformation of coordinate axes allows calculating the magnitudes of the variables corresponding to $\{\varepsilon_1, \varepsilon_2, \gamma_{12}\}$, in the directions of axes 1 and 2, by means of the expressions

$$\begin{aligned}\varepsilon_r &= f(\varepsilon_1, \varepsilon_2, \gamma_{12}, \theta_r), \\ \varepsilon_s &= f(\varepsilon_1, \varepsilon_2, \gamma_{12}, \theta_s), \\ \varepsilon_t &= f(\varepsilon_1, \varepsilon_2, \gamma_{12}, \theta_t).\end{aligned}\quad (1)$$

$\{\varepsilon_1, \varepsilon_2, \gamma_{12}\}$ is obtained on the surface of the moving jaw in P . This is a particular case of flat strain, whereupon it is possible to calculate the magnitudes of flows of $\{\sigma_1, \sigma_2, \tau_{12}\}$ at P based on the expressions (see Figure 3.b)

$$\begin{aligned}\sigma_1 &= \frac{E(v\varepsilon_2 + \varepsilon_1)}{1 - v^2}, \\ \sigma_2 &= \frac{E(\varepsilon_1 + v\varepsilon_2)}{1 - v^2}, \\ \tau_{12} &= \gamma_{12}G,\end{aligned}\quad (2)$$

where G is the shear module. The magnitude of the longitudinal stress σ_2 is used to estimate the force F_2 (see Figure 4). This is $\sigma_2 = \frac{F_2}{w \cdot h}$, where w and h is the width and the thickness of the cross section of the moving jaw, respectively. Therefore, to find the clamping force F_c between the moving jaw and the track rope, the load balancing $a \cdot F_c = b \cdot F_2$ is considered.

This force distribution can be continuously inspected and compared with a reference value (established by international standards), which is a procedure that allows to determine the behaviour of the system force, regardless of the position of the gondola and the loads it receives.

{Figure 3}

{Figure 4}

5. Calibration process of a measuring system

A calibration process is developed for the experimental tests. The process consists of two stages:

- a first stage consists of a controlled test made in quasi-static conditions and it has been performed in the workshop, i.e. then the test has been isolated to external conditions, then the test has the following features: (i) without the wind loads effect; (ii) without operating frequency, due to the air cable car is out to the commercial line; (iii) the air cable car has constant speed, $V = 5\text{m/s}$; (iv) with a constant temperature and moisture. From the signals of the strains $\{\varepsilon\}_{stat}$, a segment of data is extracted, corresponding to a characteristic inter-station trip, in which the moving jaw applies a work in ξ_0 ;
- a second stage consists of solving the FE model emulating a static test in ξ_0 load condition, analogous to the first stage of calibration process and calculating the static strains $\{\varepsilon\}_{FE}$ at P .

Then, the obtained results in each of the two stages are compared, i.e. the result from the workshop controlled test $\{\varepsilon\}_{work_{shop}}$ and the values calculated in FE $\{\varepsilon\}_{FEA}$. This allows to get a calibration coefficient $K = \{k_r, k_s, k_t\}$ (see Figure 5), which will be used later to adjust the records obtained during the inspection method to assess the journey safety of aerial cable cars.

The calibration coefficient is used to calculate the calibrated dynamic strains $\{\varepsilon\}_{dyn} = K\{\varepsilon\}_{test}$ in commercial condition, where

$$K = f(\{\varepsilon\}_{work_{shop}}, \{\varepsilon\}_{FEA}), \quad (3)$$

6. Analysis of results

Based on $\{\varepsilon(t)\}_{test}$ in all the circuit, including inter-station trips and transit within the stations, an algorithm was developed to calculate the magnitude of F_c (see Figure 5) by means of structured sequential steps that allow getting a journey safety assessment with real-time data processing and during the ropeway commercial operation. Figure 6.a shows the variation of σ_2 in two different inter-station trips, where σ_2 is a dynamical signal, because of σ_2 is a direct result of $\{\varepsilon(t)\}_{test}$ real-time data processing. Fluctuations in the magnitude are due to multiple reasons, some of them are, among others: (i) oscillation of the aerial cable car because of the wind load; (ii) variation of the gravity centre of the air car because of the movement of passengers; and (iii) fluctuations in operation speed, $V(t)$.

Figure 6.b shows the variation of σ_2 in the transit of the aerial cable car within two different stations. Here it is also seen that the magnitude of σ_2 is a stable compared with the signal σ_2 inter-station trips, however, the main fluctuations due to: (i) the disruption that occurs when entering and exiting the station due to the engagement and disengagement of the cable grip to and from the track rope; (ii) the disruption caused by the passengers when getting on and off the aerial cable car; (iii) the movement of the air car in the station, effected by an external transmission that produces vibrations.

{Figure 5}

{Figure 6}

7. Conclusions and future work

The proposed algorithm gives the possibility of automating the process of ongoing inspection of F_c , for assessing the journey safety of a passenger aerial cable car of urban transportation on an aerial ropeways.

There is a clear feasibility to implement the proposed procedure for the entire fleet of aerial cable cars of urban aerial ropeway systems, due to: (i) the sensors and data acquisition systems are widely studied for technical elements that do not represent a challenge to the current industrial sector; (ii) the costs of implementation are low in relation to the amount of information that the process may obtain from the system.

In case that F_c is found constant in normal records from a moving jaw over a period of time, and suddenly changes during the records, it could implicate a wear symptom.

The developed algorithm allows performing different types of analysis for an aerial cable transportation system, since the implementation could be targeted for different purposes:

- (i) to observe the behaviour of the components wear of the cable grip of the aerial cable car in relation to the coupling with the rope, by means of the determination of the variation of F_c level in a same aerial cable car, during a representative period of time in relation to the operation of the system in its life cycle,
- (ii) to observe the influence of environmental factors (wind load, temperature, humidity, etc.), and operation factors (passenger load, frequency of operation, etc.), using the variation of the level of F_c in a

same journey for different aerial cable cars that travel within the system;

- (iii) to establish the relationship between the variations of the magnitude of F_c force as a parameter to infer the rope wear.

The proposed algorithm is useful whereas the data logging allows getting information in terms of commercial operation, avoiding measurements that require downtime for the system inspection.

The record of the signals during a sufficient period of time allows the development of statistics that can be used for maintenance planning. This means that the proposed procedure represents the technological basis for the development of a predictive maintenance program or a based on condition maintenance for the assessment of the F_c journey safety.

The paper opens to different research fields, elements that can be considered for future publications: (i) to study of the short pulses –with high frequency components– in F_c signal; (ii) to study the cable load and stress relative to the excitation frequencies effect; (iii) to study the relationship between the F_c variation and the aerial cable car faults to identify the technical state in commercial conditions.

Appendix 1. Notation

Abbreviations, acronyms, coefficients and constants

FE	Finite Elements.
MPE	Minimum Potential Energy.
$\{b\}$	Volumetric forces.
$[D]$	Symmetric matrix stiffness of material.
$\{I_t\}$	Inertia matrix.
$\{M\}, \{P\}$	Applied punctual moments and forces, respectively.
$[N]_{(x,y,z)}$	Interpolation matrix function.
$\{t\}$	Surface unity forces.
$\{u\}, \{U\}$	Displacement vector and tensor, respectively.
$\{\sigma\}, \{\varepsilon\}$	Stress and strain tensor, respectively.
$\vec{a}_t, \vec{\rho}_t$	Translational and rotational accelerations, respectively.

E, G, ν	Elasticity, shear and Poisson modules, respectively.
F_C	Clamping Force.
K	Calibration coefficient
m_t	Moving jaw mass.
P	Measuring point.
S, V	Surface area and solid volume, respectively.
q	Number of nodes of a FE.
w, h	Height and thickness of cross section, respectively.
$W_p(u)$	Potential energy of the external forces.
$\xi_i, i = \{0, \dots, 4\}$	i -th load state.
$\Pi(u)$	Strain energy of the body.
Π_p	Total potential energy of an elastic body.

Appendix 2. Boundary FEA model conditions

{Figure 7}

{Table 2}

Appendix 3. Stress distribution

{Figure 8}

References

- Bryja, D. and Knawa, M. (2011) 'Computational model of an inclined aerial ropeway and numerical method for analyzing nonlinear cable-car interaction', *Computers and Structures*, 89, 1895–1905.
- Degasperi, F. (1999) 'Measurement of dynamic stresses on carriers with detachable grip at station entrance: LA.T.I.F. experiences and future prospects', *8th International Congress for Transportation by Rope (OITAF)*, 107–133.
- Doppelmayer, A. (1998) *Conceptual inputs for optimizing the functional efficiency of circulating monocable ropeways: project engineering, design and operation in a safety management control loop based on incident analysis*, WIR Public, Austria.
- Hoffmann, K. (2006) 'Recent developments in cable-drawn urban transport systems', *FME Transactions*, 34, 4, 205–212.
- Innova, Patent GmbH (2002) 'Device for checking the clamping force of the coupling assembly for a movable transport unit of a cableway installation', *Australian Patent Office*, Patent Nr. AU2003203595(A1), Australia.
- Konieczny, J., Pluta, J., Podsiadło, A. (2008) 'Technical condition diagnosing of the cableway supports' foundations', *Acta Montanistica Slovaca*, 13, 1, 158–163.
- Liedl, S. (1999) 'Motions and forces in the rope system of aerial ropeways during operation', *8th International Congress for Transportation by Rope (OITAF)*, 381–392.

- 1
2
3 Mizuma, T. (2004) 'Recent urban transport technologies and assessments', *Japanese*
4 *Railway Engineering*, 152, 5–10.
5
6 Petrova, R., Karapetkov, St., Dechkova, S. and Petrov, Pl. (2011) 'Mathematical
7 Simulation of Cross-Wind Vibrations in a Mono-Cable Chair Ropeway',
8 *Procedia Engineering*, 14, 2459–2467.
9
10 Pomagalski, S.A. (1996) 'Device for remote measurement of clamping force of cable
11 car or chair lift support cable clamp', *Institut National de la Propriété*
12 *Industrielle*, Patent Nr. FR2750764-A1, France.
13
14 Sever D. (2002) 'Some new methods to assure harmonisation of sustainable
15 development of mountain resorts ropeway', *Promet-Traffic-Traffico*, 14, 5,
16 213–220.
17
18
19
20
21
22
23
24
25
26
27
28
29
30
31
32
33
34
35
36
37
38
39
40
41
42
43
44
45
46
47
48
49
50
51
52
53
54
55
56
57
58
59
60

1
2
3 Figure 1. Components of the aerial cable car coupling assembly.
4

5
6 Figure 2. Description of the measurement point.
7

8 Figure 3: Strain and stress axes.
9

10 Figure 4. Description of the measurement point P .
11

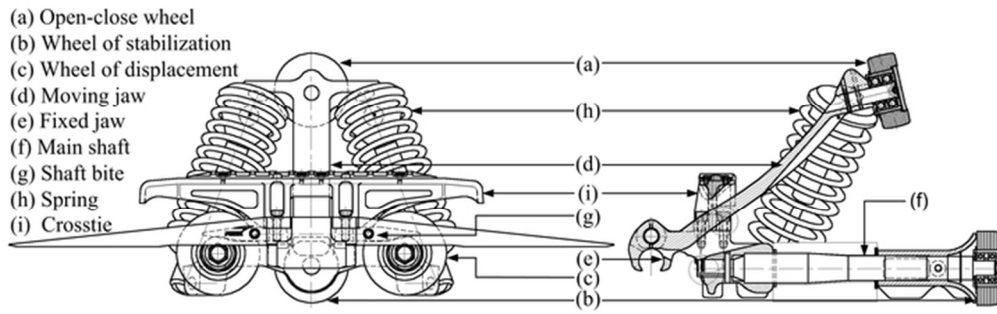
12 Figure 5. Algorithm for the proposed inspection method.
13

14 Figure 6. Stress results σ_2 on the point P .
15

16
17 Figure 7. FE boundary conditions.
18

19 Figure 8. Moving jaw stress distribution.
20
21
22
23
24
25
26
27
28
29
30
31
32
33
34
35
36
37
38
39
40
41
42
43
44
45
46
47
48
49
50
51
52
53
54
55
56
57
58
59
60

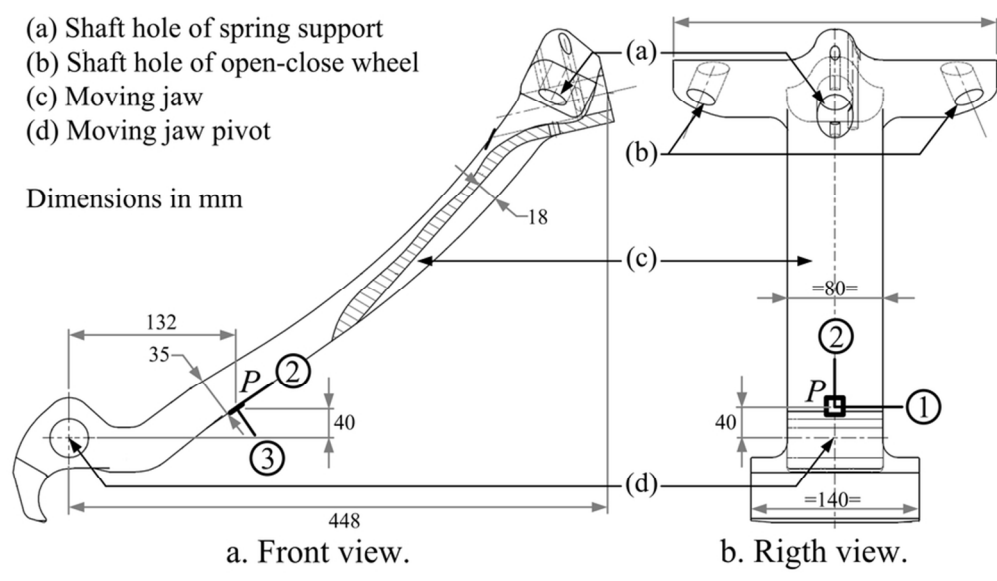
1
2
3
4
5
6
7
8
9
10
11
12
13
14
15
16
17
18
19
20
21
22
23
24
25
26
27
28
29
30
31
32
33
34
35
36
37
38
39
40
41
42
43
44
45
46
47
48
49
50
51
52
53
54
55
56
57
58
59
60



60x18mm (300 x 300 DPI)

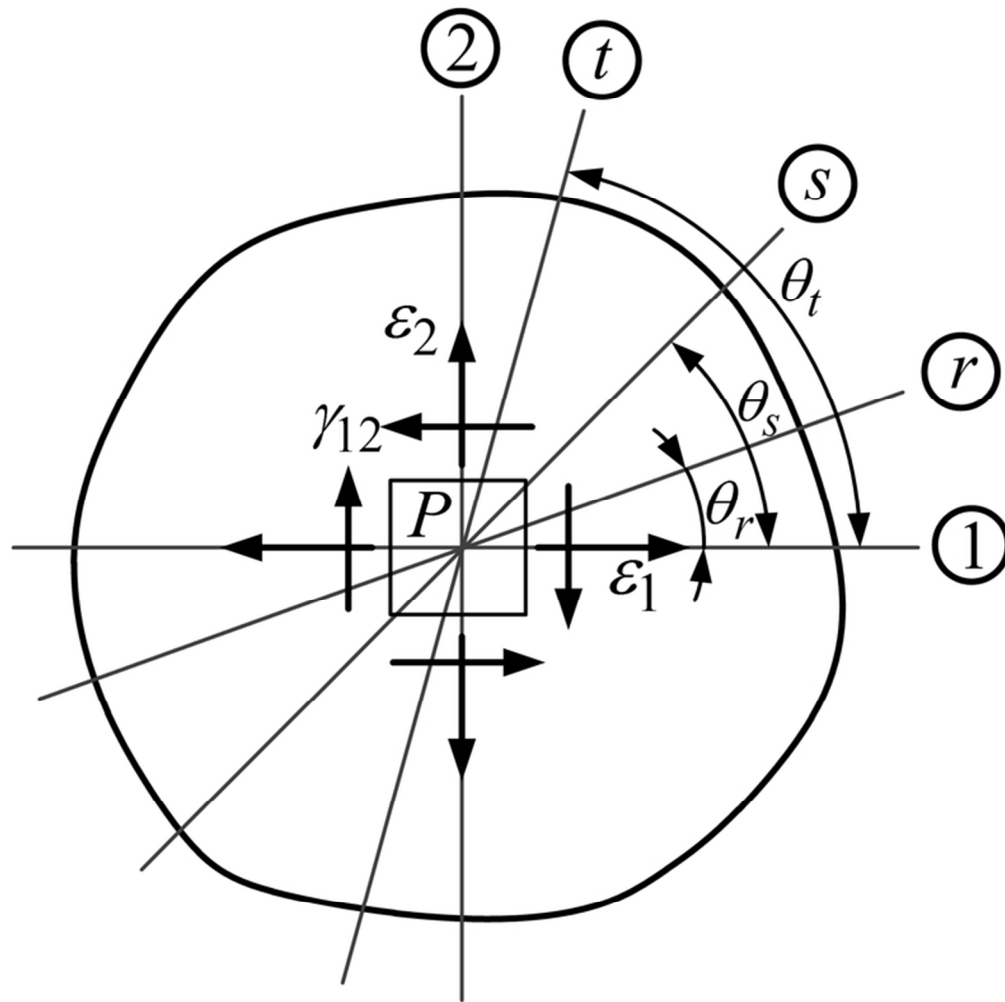
Peer Review Only

1
2
3
4
5
6
7
8
9
10
11
12
13
14
15
16
17
18
19
20
21
22
23
24
25
26
27
28
29
30
31
32
33
34
35
36
37
38
39
40
41
42
43
44
45
46
47
48
49
50
51
52
53
54
55
56
57
58
59
60



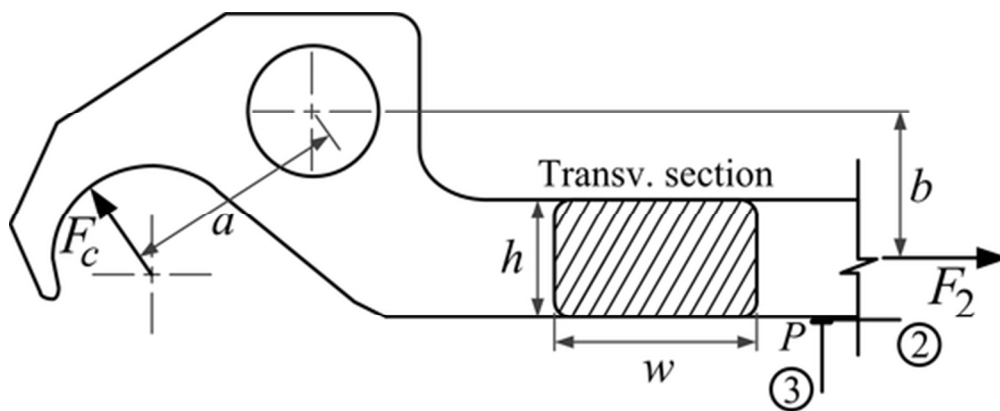
83x47mm (300 x 300 DPI)

Review Only



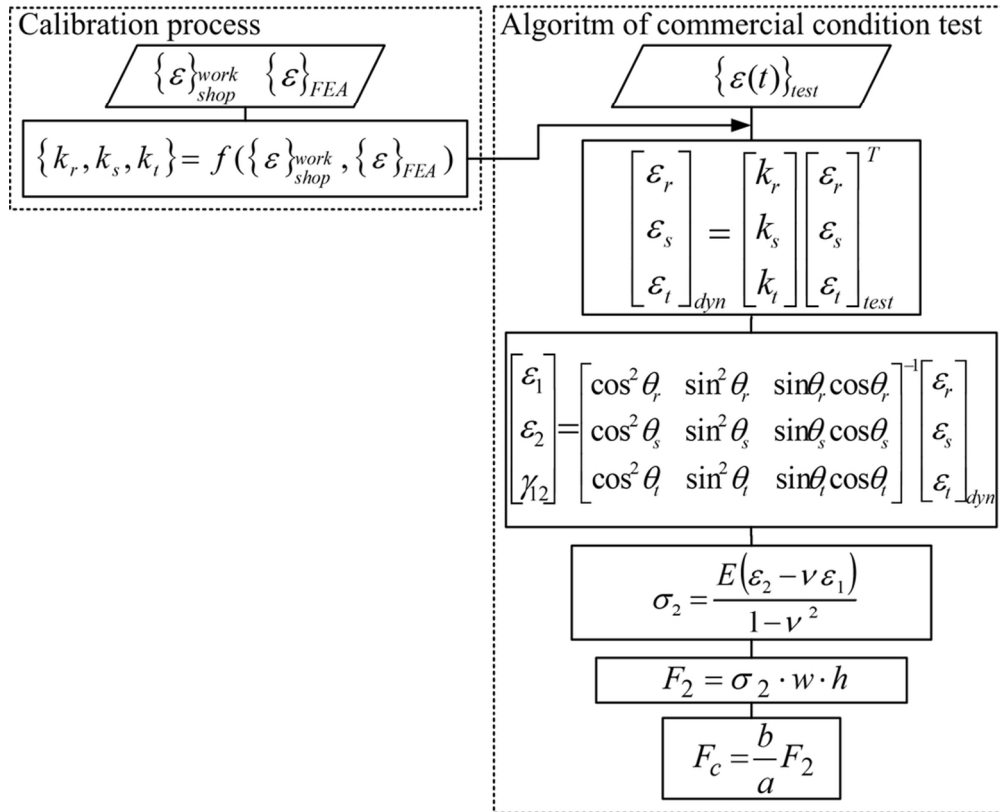
66x66mm (300 x 300 DPI)

1
2
3
4
5
6
7
8
9
10
11
12
13
14
15
16
17
18
19
20
21
22
23
24
25
26
27
28
29
30
31
32
33
34
35
36
37
38
39
40
41
42
43
44
45
46
47
48
49
50
51
52
53
54
55
56
57
58
59
60



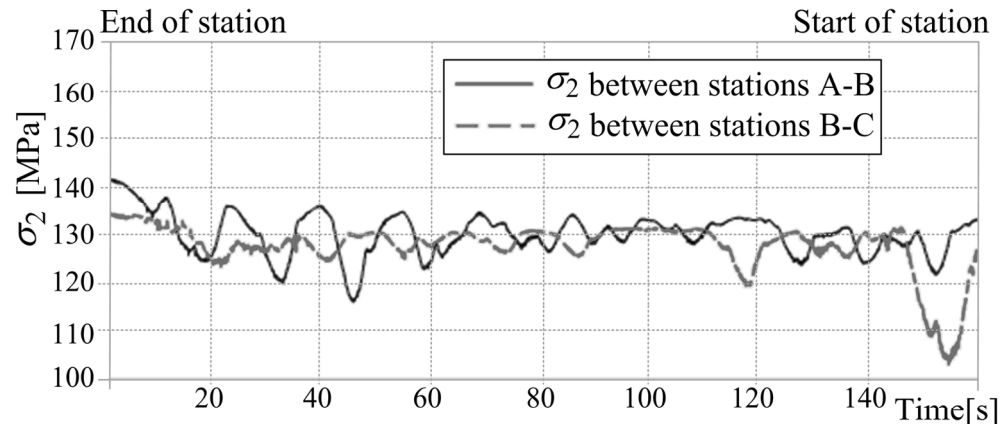
47x19mm (300 x 300 DPI)

Peer Review Only

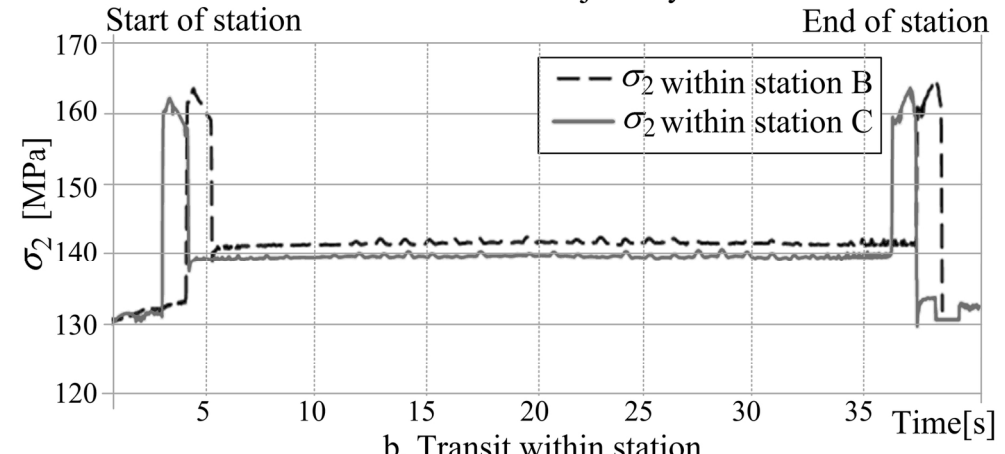


91x74mm (300 x 300 DPI)

1
2
3
4
5
6
7
8
9
10
11
12
13
14
15
16
17
18
19
20
21
22
23
24
25
26
27
28
29
30
31
32
33
34
35
36
37
38
39
40
41
42
43
44
45
46
47
48
49
50
51
52
53
54
55
56
57
58
59
60



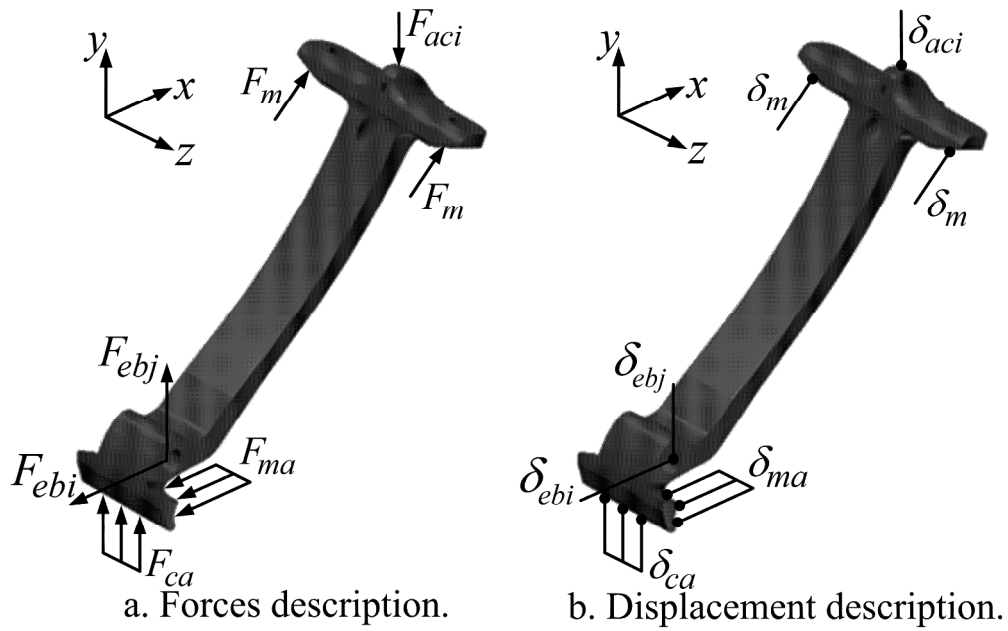
a. Inter-station journey



b. Transit within station

156x145mm (300 x 300 DPI)

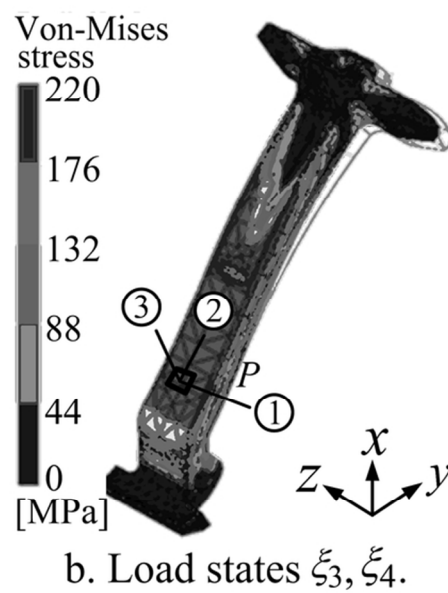
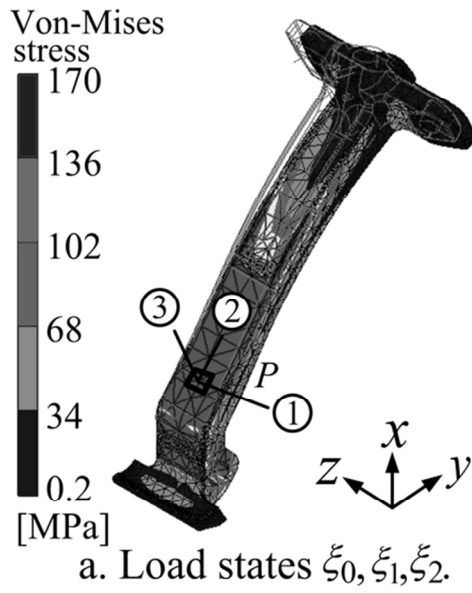
Only



258x164mm (300 x 300 DPI)

1
2
3
4
5
6
7
8
9
10
11
12
13
14
15
16
17
18
19
20
21
22
23
24
25
26
27
28
29
30
31
32
33
34
35
36
37
38
39
40
41
42
43
44
45
46
47
48
49
50
51
52
53
54
55
56
57
58
59
60

1
2
3
4
5
6
7
8
9
10
11
12
13
14
15
16
17
18
19
20
21
22
23
24
25
26
27
28
29
30
31
32
33
34
35
36
37
38
39
40
41
42
43
44
45
46
47
48
49
50
51
52
53
54
55
56
57
58
59
60



79x48mm (300 x 300 DPI)

Review Only

Table 1. General features of the transport ropeway system.

General features	System line		
	K-line	J-line	L-line
Length of the plot [m]	2 072	2 789	4 595
Capacity [pass/hour]	3 000	3 000	1 200
Heighth's difference [m]	399	309	470
Medium slope [%]	20	12	15
Maximum slope [%]	49	43	58
Commercial speed [m/s]	5	5	6
Gondola cap. [pas]	10	10	10
Quant. stations [ud.]	4	4	2
Quant. tows [ud.]	20	31	25
Quant. vehicles [ud.]	90	119	27
Dist. between vehicles [m]	60	60	340
Frequency [s]	12	11.5	65
Energy	Electric (central energetic source) and solar (lighting inside the vehicle)		

Table 2. FE boundary conditions.

Load	Load states, ξ_i				
	ξ_0	ξ_1	ξ_2	ξ_3	ξ_4
F_{ACI} [kN]	0.000	0.000	0.000	9.270	-12.358
F_m [kN]	8.627	8.627	8.627	8.704	16.485
F_{ebi} [kN]	76.908	76.908	76.908	6.088	-22.316
F_{ebj} [kN]	21.580	20.147	20.991	6.037	-7.923
F_{ma} [kN]	82.887	82.887	82.887	0.000	0.000
F_{ca} [kN]	6.468	4.949	4.949	0.000	0.000

For Peer Review Only

Amendments to Reviewers for Authors

Journal: Journal of Transportation Safety & Security

Title: Journey safety assessment to urban aerial ropeways transport systems based on continuous inspection during operation

Manuscript ID: UTSS-2013-0036

Reviewer 1

Manuscript recommendations:

1. (Section 3.1) Posing the static model of linear elasticity – instead of writing this commonly known theory, it will be better to explain why linear static analysis is chosen and to emphasize of the assumptions.

This element has been broadened in the Manuscript

2. (Section 3.1 & 3.2) Probably items 3.1. and 3.2. can be united, with a stronger focus on the developed FE analysis, especially compared to already existing mathematical models for calculation of the clamping force. There are mathematical models, which calculate the vibrations at the clamping point, respectively the clamping force, using FEM.

This concept has been empathized in the Manuscript

3. (Section 3.2) It is worthy to be mentioned the used software.

The Manuscript has been corrected: ... using the integration algorithms developed by Ansys.

4. (Section 3.2) Check the reference [15] (1.24, p.8).

The Figure has been corrected

5. (Section 3.2) As this is not reasonable Figure 7 (1.26, p.8) to be cited before Fig. 3 to 6, it is better the order of figures to be reconsidered.

The Figure has been corrected

6. (Section 3.3) Explain in more details the criteria of choosing the measuring point to increase the strengths of the study.

7. *This element has been broadened in the Manuscript*

8. (Section 4) Determination of measuring system under operating conditions: Explain the exact meaning of ϵ_i and K_i . A brief explanation of the calibration coefficients K_i is available later (1.14, p.11), while the reader expects to read it, when workflow is discussed.

This element has been broadened in the Manuscript

9. (Section 4) Underlining the close real-time interaction between measurements and calculations, which according to me is one of the basic strengths of the research.

This concept has been empathized in the Manuscript

10. (Section 4) Another definite strength of the system is that the measurements are made during the ropeway operation and it is worthy to be emphasized

This concept has been empathized in the Manuscript

11. (Section 5) It will be better if some numerical data can be provided. The calibration coefficients K_i are calibrated at an operating velocity of 6m/s. Do they preserve their values if the velocity is decreased to 5m/s?

The speed of 6m/s was a typing mistake, the Manuscript has been corrected

12. (Section 6) As this is the most important part of the research it will be better if some more data can be provided. The cited experiments can involve the three lines (K, L and J), which are described as a part of the model and which data is provided in table 1.

This element has been broadened in the Manuscript

Illustrations recommendations:

13. Figure 2: Description of the measuring point – 2a: the left view matches more to the other two views than the right view; further the place of measuring point will be better viewed. Annotation 3, which is normal to the plane of the measured strains, is better to be omitted instead of to complicate the view.

The Figure has been corrected

14. Figure 3: Strain and stress axes – 3a: check the ark for θ_k ; 3b is commonly known and is better to be omitted.

The Figure has been corrected

15. Figure 4: Description of the measuring point P – I suggest the title of that figure to be reconsidered, as far as measuring point P is not even visible in the figure.

The Figure has been corrected

16. Figure 5: Algorithm for the proposed inspection method.- It is not clearly stated what kind of strains ϵ_r' , (ϵ_r , ϵ_s , ϵ_t).

17. Figure 6: Stress results σ_{-} on the point P – there are no values for time, which reduces the quality of the measured ϵ_s' and ϵ_t' are, what is the definition of the coefficients K_r , K_s and K_k ; hence what is the relation $\epsilon_i' = f$ data and embarrasses the assessment.

The Figure has been corrected

18. Figure 7: (page 23) – No title, the annotation δ_{aci} in displacement description to be corrected; δ_{aci} – no arrow to point the direction. The presentation of displacements δ_{ca} and δ_{ma} , which correspond to distributed linear loads F_{ca} and F_{ma} , is not quite clear : are there three different values, whose average value is given in the table 2 or only one displacement value is provided?

The Figure has been corrected

19. Figure 8: (page 24) – No title; the figure should be made brighter to better its visibility. Is this the plots for the highest dynamic values of the forces for all the simulated cases? Why if we can measure the strains versus time and as a result of the proposed algorithm to calculate F_C , we develop static linear analysis instead of transient analysis for $F_C(t)$ and thus to calculate maximum von Mises stresses.

The Manuscript has been corrected

Tables recommendations:

20. In table 2: the data about δ_i is either 0.000 or missing (dash). Thus either the units of displacement or the existence of these lines should be reconsidered as they provide no information.

The Table has been corrected

Appendix recommendations:

21. Abbreviations, formulas, units: All used formulas are familiar and clear; K_i abbreviation is not explained

The Appendix has been corrected

Reviewer 2

Comments to the Author:

Work submitted for publication and reviews is worth publishing. It includes many aspects of an innovative approach to research and development results. It is difficult to assess the contribution of individual authors in the development of the material. He deserves publication and distribution.

Reviewer 3

Comments to the Author

I accepted the publication but I recommend the corrections I sent you.

Bibliography leaf - Observations:

1. ... Castañeda ^{a*} Heredia* ¿Why *?

It is a footnote related to the corresponding author (see footline)

2. Why you've to repeat six times the addresses in EAFIT?

The Manuscript has been corrected.

3. In English it's COLUMBIA, isn't it?

Colombia, please see the following link (oxford Dictionary):

<http://www.oxforddictionaries.com/es/definicion/ingles/Colombia?q=colombia>

Columbia, please see the following link (oxford Dictionary):

<http://www.oxforddictionaries.com/es/definicion/ingles/Columbia?q=columbia>

Abstract - Observation:

4. ...of mass... of the type of passengers of the detachable... (four times of!)

The Manuscript has been corrected: ...of mass transportation, type of detachable...

Keywords - Observation:

5. Keywords: aerial cable car OR funicular, ~~infrastructure design, mathematical modeling, simulation~~, urban ropeway system.

The Manuscript has been corrected:

Keywords: aerial cable car or funicular, cable grip, journey safety, strain gauges, urban ropeway system.

Introduction - Observations:

6. ...safety of the service, ... inspect periodically the...

The Manuscript has been corrected: ...safety of the service, (...) inspect periodically the

7. ...routines must include....

The Manuscript has been corrected

8. ...of the force F_c at the point

The Manuscript has been corrected.

9. The state of the art..., so it is a critical system:

- In Document FR2750764 a...
- Document AU2003203595A1...

The Manuscript has been corrected.

10. None ... devices complies with...

The Manuscript has been corrected.

11. ...system has to be stopped

The Manuscript has been corrected.

12. OJO: En su caso no vaya a mencionar ... ~~demands great resources (...), and~~ requires porque algo barato de pronto es menos.

The Manuscript has been corrected.

13. ...operation of the system; ~~and~~ (ii) the...

The Manuscript has been corrected.

14. ...which record a reliable signal,

The Manuscript has been corrected: ...which record reliable signals,

Description of the object of study- Observations:

15. ...passenger air cars which... what air cars: aerial cable car, funicular, gondola lift?

The Manuscript has been corrected: ...passenger aerial cable cars which...

16. ...belong to a fleet consisting ... cable grip, which operates

Ninguna información útil para el lector

El texto ha sido corregido.

17. (Sever, 2002), it has been ... by Pomagalski/France, since 2004, serving continuously 360 days a year, 7 days a week, 20 hours a day.

The Manuscript has been corrected

18. This is the first time in the world that used an aerial cable was used for urban purpose,...

The Manuscript has been corrected

19. so that soon it will be become the ... with highest level of demand in the world, in terms ...

The Manuscript has been corrected

20. 2011). The cable grip is made up of 52 parts. Figure 1 shows the main elements of the cable grip, defined.

The Manuscript has been corrected

21. The work development focuses

The Manuscript has been corrected

22. material with HB350-390 hardness and has a resistance to stress of 850 MPa, according to the manufacturer material specifications.

The Manuscript has been corrected

23. ...load states applied exercised to the...

The Manuscript has been corrected

24. ... state in which __ the open-close-wheel

The Manuscript has been corrected

Determination of the inspection point on the coupling device – Observations:

25. ...is done by through an analysis ... at each of the load states ξ_i ; $i = \{0, \dots, 4\}$.

The Manuscript has been corrected

26. ...was performed with Finite Elements Method (FE) using

The Manuscript has been corrected

27. ...in each of load states, so that

The Manuscript has been corrected

28. OJO: Me parece que la carga en ξ_0 es dinámica. Deben decir algo al respecto, utilizando un modelo estático

The Manuscript has been corrected:

...the load state ξ_0 is sensitive to external conditions (Degasper, 1999): (i) the terms and conditions of operation –live loads, operation frequency–; (ii) environmental conditions –wind loads, temperature, moisture, corrosion, etc.–; and (iii) system availability. However, the load state ξ_0 can be considered a quasi-static load in the event of the load state ξ_0 is made in a controlled tests, which has been performed in quasi-static conditions, i.e. then the test has been isolated to external conditions, then the test has the following features: (i) a null live load; (ii) a constant travel speed; (iii) with a negligible wind load; (iii) with a constant temperature and moisture.

Posing the static model of linear elasticity – Observations:

29. ...model with EF FE allows...

The Manuscript has been corrected

30. Formulas deberían tener una enumeración.

El texto ha sido corregido.

31. ...elastic body; Π , the strain...

The Manuscript has been corrected

32. Formula (2) es falsa!!!

The Manuscript has been corrected

33. ...tensor, and $\{\epsilon\}$ the strain tensor.

The Manuscript has been corrected

- 1 34. ...the E and ν constants, which represent the module of elasticity and the module of Poisson, respectively.
 2
 3 *The Manuscript has been corrected*
 4 35. ...analysis starts with the ... is built with the... *The Manuscript has been corrected*
 5
 6 36. ...material; (iv) the stress that are *The Manuscript has been corrected*
 7
 8 37. ...for each ξ_i it is... *The Manuscript has been corrected*
 9
 10 38. ...denote translational and rotational acceleration... *The Manuscript has been corrected*
 11 39. Figure 7 tiene un error en b) *The Manuscript has been corrected*
 12 40. ~~The development ... 2.5mm.~~ *The Manuscript has been corrected*
 13 41. Therefore ~~OUR~~ the task will focus *The Manuscript has been corrected*
 14 42. Force at ~~such~~ these load states. *The Manuscript has been corrected*
 15 43. ...system; (iii) the measuring... *The Manuscript has been corrected*
 16 44. A measuring ~~experimental~~ arrangement is set at point P to...
 17
 18
 19
 20
 21 *The Manuscript has been corrected*

22 **Development of a measuring system under operating conditions – Observations:**

- 23 45. ...(see Figure 3.a). This... *The Manuscript has been corrected*
 24 46. ...surface of the moving jaw in the point P. *The Manuscript has been corrected*
 25 47. ...recorded values $\{\epsilon_r, \epsilon_s, \epsilon_t\}$ are... *The Manuscript has been corrected*
 26 48. ...means of the ~~following~~ expression *The Manuscript has been corrected*
 27 49. ...surface of the moving jaw in P. *The Manuscript has been corrected*
 28 50. ...based on the ~~following~~ expressions *The Manuscript has been corrected*
 29 51. ...stress σ_2 is used ...where w and h is... *The Manuscript has been corrected*
 30 52. El módulo de cizallamiento G no está explicado *The Manuscript has been corrected*
 31 53. Me parece que las magnitudes de deformación en las formulas no coinciden con los de la Figure 4.
 32
 33
 34
 35
 36
 37 *Sin comentario*

38
 39 **Calibration of measuring system – Observation:**

- 40 54. ...condition ~~and~~; *The Manuscript has been corrected*

41
 42
 43 **Analysis of results – Observations:**

- 44 55. Based on $\{\epsilon_r(t), \epsilon_s(t), \epsilon_t(t)\}$ in all the... *The Manuscript has been corrected*
 45 56. No veo $\sigma_2 \approx const$ en inter-station trip! En mi opinión es una magnitud dinámica. ¿Qué sucede cuando
 46 las variaciones de σ_2 son demasiado grandes?
 47
 48
 49 *The Manuscript has been corrected:*
 50
 51 *... σ_2 is a dynamical signal because of σ_2 is a direct result of $\{\epsilon(t)\}_{test}$ data processing.*
 52 57. ...of the air car _____ because ... passengers; ~~and~~ ... fluctuations in operation speed; V.
 53
 54 *The Manuscript has been corrected*
 55 58. ...air car; ~~and~~ (iii) the movement *The Manuscript has been corrected*
 56 59. También los pulsos cortos representan cargas dinámicas. ¿Qué sucede debido a las altas frecuencias
 57 incluidas? ¿De qué tipo de transmisión externa, produciendo vibraciones están hablando?
 58
 59
 60 *Ésta observación es tema de otro estudio, por lo tanto, puede ser considerado en otra publicación.*

60. Analizar frecuencias de las perturbaciones ¿Cómo actúan las vibraciones de tensión de alta frecuencia sobre un cable? Analizar publicaciones

Ésta observación es tema de otro estudio, por lo tanto, puede ser considerado en otra publicación.

Conclusions and future work – Observations:

61. ...due to: (i) the sensors and data ...; and (ii) the costs ... are ~~cheap~~ low in relation...

The Manuscript has been corrected

62. Change frase → In case that F_c in normal records ... is found constant, and during the records suddenly changers, this could implicate a symptom of wear.

The Manuscript has been corrected

63. Explicar (con cuidado) que todavía faltan datos y experiencias reales para poder interpretar la variación de F_c como resultado de una falla.

This element has been broadened as a future work.

64. ...system; and

The Manuscript has been corrected

65. ...program or ____ based on condition maintenance ____, for the assessment...

The Manuscript has been corrected

Appendix 1. Notation – Observations:

66. Falta G

The notation has been corrected

67. $\vec{a}_t, \vec{\rho}_t$ Translational and rotational accelerations, respectively.

The notation has been corrected

68. E, G, ν Elasticity, shear and Poisson modules, respectively.

The notation has been corrected

69. ν, ν , mirar texto arriba para la constant de Poisson (letras distintas)

The notation has been corrected

70. $\xi_i, i = \{0, \dots, 4\}$

The notation has been corrected

71. Π falta subíndice para strain energy

The notation has been corrected

References – Observations:

72. Literatura básica:

~~Bathe, K.J. (1996) *Finite Element Procedures*, Prentice Hall, New Jersey, USA.~~

~~Genta, G. (2009) *Vibration Dynamics and Control*, Springer Science Business, Torino, Italy.~~

~~Martinod, R., Betancur, G., Castañeda, L. (2012) Identification of the technical state of suspension~~

~~elements in railway systems, *Vehicle System Dynamics*, 50, 1121–1135.~~

~~O'Neil, P.V. (2003) *Advanced Engineering Mathematics*, Thomson, Australia.~~

~~Ruiz, O. and Cadavid, C. (2008) *Geometric Functions in Computer aided Geometric Design*,~~

~~Zienkiewicz, O.C. and Morgan, K. (2006) *Finite Elements & Approximation*, Dover Publications, USA.~~

The reference has been corrected

73. Liedl no aparece en el texto de arriba

The reference has been corrected

1
2
3
4
5
6
7
8
9

Associate Editor

Finally, I also note of particular concern is the English Grammar will require serious revision in your submission. This is despite Reviewer 1 indicating the English Grammar is good. All three reviewer's native language is not English. We will require that you seek the assistance of a professional English proof reader whose native language is English and who is a competent technical manuscript proof reader. Unless this is done in a satisfactory and professional manner, the paper cannot be published.

The English grammar and the typing errors has been corrected

10
11
12
13
14
15
16
17
18
19
20
21
22
23
24
25
26
27
28
29
30
31
32
33
34
35
36
37
38
39
40
41
42
43
44
45
46
47
48
49
50
51
52
53
54
55
56
57
58
59
60

For Peer Review Only